ScienSage

Journal of Advanced Scientific Research

Available online through https://sciensage.info

ISSN
0976-9595
Research Article

SYNTHESIS OF Fe_3O_4-Ag CORE SHELL NANOPARTICLES USING *CINNAMOMUM VERUM* BARK EXTRACT AND REMOVAL OF METHYL ORANGE FROM AQUEOUS MEDIA

Priya Kumari*, Masood Alam

Department of Applied Sciences & Humanities, Faculty of Engineering and Technology, Jamia Millia Islamia, New Delhi, India

**Corresponding author: priyakm2102@gmail.com*

Received: 21-03-2023; Accepted: 12-04-2023; Published: 30-04-2023

 https://doi.org/10.55218/JASR.202314407

ABSTRACT

Green synthesis of Fe_3O_4-Ag core shell nanoparticles (CSNPs) was performed using *Cinnamomum verum* bark extract (CVBE) as the green solvent, reducing agent and capping agent. Aqueous solutions of $AgNO_3$, $FeCl_3.6H_20$ and CH_3COONa were used for the synthesis. The first formation of Fe_3O_4-Ag CSNPs was observed within 10 minutes of the reaction time. The result recorded from UV-Vis spectroscopy, Fourier Transform infrared spectroscopy (FTIR) and Energy dispersive spectroscopy (EDS) favours the biosynthesis and characterization of Fe_3O_4-Ag CSNPs. Scanning electron microscopy (SEM) reveals that the shape is nearly spherical and Transmission electron microscopy (TEM) confirms the shape as spherical and minimum size achieved is 19 nm. The capability of synthesised Fe_3O_4-Ag CSNPs for adsorption of methyl orange (MO) was tested in batches. It was observed that the process is pH dependent with maximum adsorption occurring at pH 6. The adsorption equilibrium was achieved after 120 min of contact time. The data observed was fitted one by one to three different isotherm models, viz., Langmuir, Freundlich and Temkin isotherm model to find the mode of adsorption. The process was best described by Langmuir isotherm. The adsorption kinetics was further analysed by using the pseudo-first-order, pseudo-second-order and the Weber-Morris diffusion model on adsorption data. The kinetic data of this adsorption obeyed pseudo-second-order rate equation.

Keywords: Adsorption, SEM, TEM, CSNPs.

1. INTRODUCTION

Many industries, like textiles, packaging, etc., use various dyes to colour their products and produce humongous volumes of waste water having high contamination of toxic dyes. Dyes are major contributors of the effluents of these industries, whose presence in water is highly undesirable even in very small quantities [1]. Most of the dyes are non-biodegradable and are hazardous to health, food and aquatic biota [2]. Most of the dyes, along with their metabolites are highly toxic, mutagenic and carcinogenic [3, 4]. Hence, removal of dyes from water is of great significance. Amongst the various methods and procedures [5-8] available for removing dyes from water include sedimentation [9], filtration [10], chemical treatment [11-13], oxidation, electrochemical methodology [14, 15]. Additionally, other than the above mentioned methods, adsorption is the most widely accepted method due to its effectiveness over wide range of chemical compounds, all the while, keeping the process simple and easy [16-26]. In the recent years, nanoparticles have come up as one of the best adsorbents due to their unique physical & chemical properties and high specific surface area.

The nanotechnology, basically, encompasses chemistry, biology, physics and material science [27]. It dwells upon and uses the concepts of all these fields and creates an amalgam to develop therapeutic nano sized particles which find applications in various fields like robotics [28], medicine [29], cosmetics [30], food industry, textile industry [31], waste water treatment, etc.

Nanoparticles are the nano-scale analogues of nobel metals. These nano-scale versions of nobel metals have gained the researchers' attention in recent decades and a lot of work is being done in the direction of developing better and eco-friendly methods of producing these nanoparticles.

Green nanotechnology is the branch of nanotechnology that studies the production of functional nanoparticles of Nobel metals like Silver, Gold, Zinc, etc. and uses

Green Synthesis for producing these nanoparticles [32-34].

Green synthesis is the method of manufacturing the nanoparticles using such reagents so that the entire process doesn't have any hazardous by-product. There are a huge number of physio-chemical methods for synthesis of Ag-NPs available in the literature [35-38] but these methods, mostly, involve various chemicals and the solvent is mostly toxic to human health because these processes use carcinogenic materials for preparation of nanoparticles. On the other hand, the biological methods, which use fungi, bacteria, polypeptides, proteins, nucleic acids and plant extracts, are very simple, affordable, non-toxic and eco-friendly. These methods can be used to synthesize nanoparticles within acceptable size range and morphology [39-40].

The silver nanoparticles in particular, are very well known for their anti-microbial properties [41-42] and are being used in medical industries widely. They have highly efficient anti-bacterial properties [43] and used in cosmetics, paints and textile industries [44-45]. Approximately 500 tons of Ag-NPs are produced annually worldwide [46]. This shows the extent of usage of Ag-NPs nowadays. The Ag-NPs are amongst the most effective adsorbents that the researchers have been using to treat the dye contamination in the water. In view of the above, it will be advantageous to develop easy and eco-friendly methods for synthesis of Ag-NPs so as to use them to efficiently treat the dye contaminated waste water. The Ag-NPs can be synthesised through numerous chemical methods available in the literature but each method has its inherent limitations and disadvantages which creates a continuous need to improve the existing methods or to develop new methods of Green Synthesis of Ag-NPs.

The current study presents the detailed process of Green Synthesis of Fe_3O_4-Ag CSNPs using *Cinnamomum verum* bark extract and further applying those synthesized nanoparticles for the removal of methyl orange from aqueous solutions using adsorption.

2. METHOD AND MATERIALS

2.1. Material

All the chemicals used in the synthesis were of analytical reagent grade. To perform course of synthesis doubly distilled water was used. Ferric chloride hexa hydrate ($FeCl_3.6H_20$), methyl orange ($C_{14}H_{14}N_3NaO_3S$), silver nitrate ($AgNO_3$), and sodium acetate (CH_3COONa) were purchased from Sigma Aldrich. The dried *Cinnamomum verum* bark (CVB) was purchased from nearby local market.

2.2. Preparation of *Cinnamomum verum* bark extract (CVBE)

As soon as the CVB was purchased from local market, it was washed first with doubly distilled water to eliminate impurities. Further, it was sundried to completely remove the moisture. The bark was broken into small pieces using mortar pestle and then turned into powdered using a mixer. To get the uniform size of the particles the powder was sieved using BSS 72 mesh size. Further, 25gm of CVB powder was added to 100 ml of distilled water in a 500 ml Erlenmeyer flask, and then boiled for 10 min.

2.3. Bio-synthesis of Nano-scale Fe_3O_4-Ag particles

An ecofriendly method was applied to synthesize Fe_3O_4-Ag CSNPs using CVBE. Firstly, 40 ml of CVBE was taken in 250 ml round bottom flask, and then 40 ml of 1M $FeCl_3.6H_20$ and 40 ml of 0.5M CH_3COONa solutions were added. The mixture was then placed on magnetic stirrer at 80°C for 5 min and 40 ml aqueous 10 mM $AgNO_3$ was added, further heating was done for 2 hours with vigorous stirring. The biological groups like carbohydrates and polyphenols present in CVBE act as reducing as well as capping agents in the synthesis. The solution then turned black with precipitate at the bottom indicating the formation of Fe_3O_4-Ag CSNPs. The resultant emulsion was then centrifuged and the nanoparticles obtained were washed several times using ethanol. Washed Fe_3O_4-Ag CSNPs were dried in oven at 90°C overnight. Fe_3O_4-Ag CSNPs were sent for characterization.

2.4. Characterization

Several techniques were used to characterize biogenically synthesized Fe_3O_4-Ag CSNPs. UV-Vis spectroscopy was performed within 1 hour of synthesis using U3900 UV-Vis spectrophotometer for the confirmation of synthesis of Fe_3O_4-Ag CSNPs. Adsorption studies of MO were also done by using UV-Vis spectroscopy. The infrared spectroscopy was performed using Tensor 37 FTIR spectrophotometer. The shape and size of the nanoparticles were studied using electron microscopy, FEI Nova NanoSEM 450 electron microscope was used for SEM analysis and Technai G2 30 S Twin electron microscope was used

for TEM analysis. EDX spectra were recorded on Bruker Nano GmBHXFlash SVE III to know the constituents of Fe_3O_4-Ag CSNPs.

2.5. Adsorption study

Adsorption study of MO using Fe_3O_4-Ag CSNPs as nano adsorbent was performed considering four variables, viz., time, pH, adsorbate concentration (MO concentration) and adsorbent dose. UV-Vis spectroscopy was used to record absorbance of reaction mixtures, during batch experiments. The spectrum was recorded at 465 nm. Data recorded was fitted to isotherm models and kinetic equations to explain the adsorption mechanism in batch experiments.

3. RESULTS AND DISCUSSIONS

3.1. Characterization of Fe_3O_4-Ag CSNPs

To confirm the formation of nanoparticles, UV-Vis spectroscopy was done. In the previous studies, nanoparticles showed sharp peaks between 420 nm to 450 nm but in present study the peak shifted to 525 nm. This is due to the fact that surface plasmon resonance (SPR) depends upon the particles size and the dielectric medium surrounding the Ag nanoparticles which leads to shift in frequency. This shift suggests that there is a formation of fine layer of Fe_3O_4 on the core of silver and hence the synthesis is successful. Fig. 1 shows the UV-Vis spectra of Fe_3O_4-Ag CSNPs.

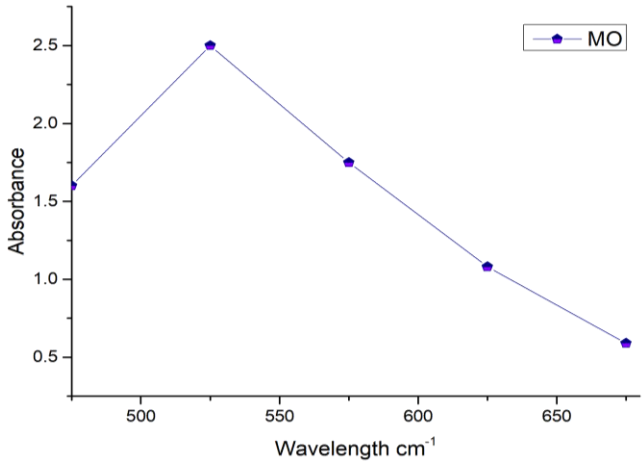

Fig. 1: UV-Vis spectrum of Fe_3O_4-Ag CSNPs

Fe_3O_4-Ag CSNPs were further characterized by using FTIR spectroscopy knowing the fact that the strength of adsorption depends upon concentration. The FTIR spectrum of Fe_3O_4-Ag CSNPs is given in Fig. 2. The peak present at 3325 cm^{-1} reveals the presence of (O−H). Other significant peaks were at 1619 cm^{-1} (C=O stretching), 1422 cm^{-1} (aromatic C=C stretch), 1088 cm^{-1} (C−O stretch) of alcohols, carboxylic acid, ethers and esters. Peaks present at 884 cm^{-1}, 782 cm^{-1}, 638 cm^{-1} shows (=C−H bending). The complex nature of the adsorbent can be clearly deduced from the various absorption peaks of the functional groups in the spectrum.

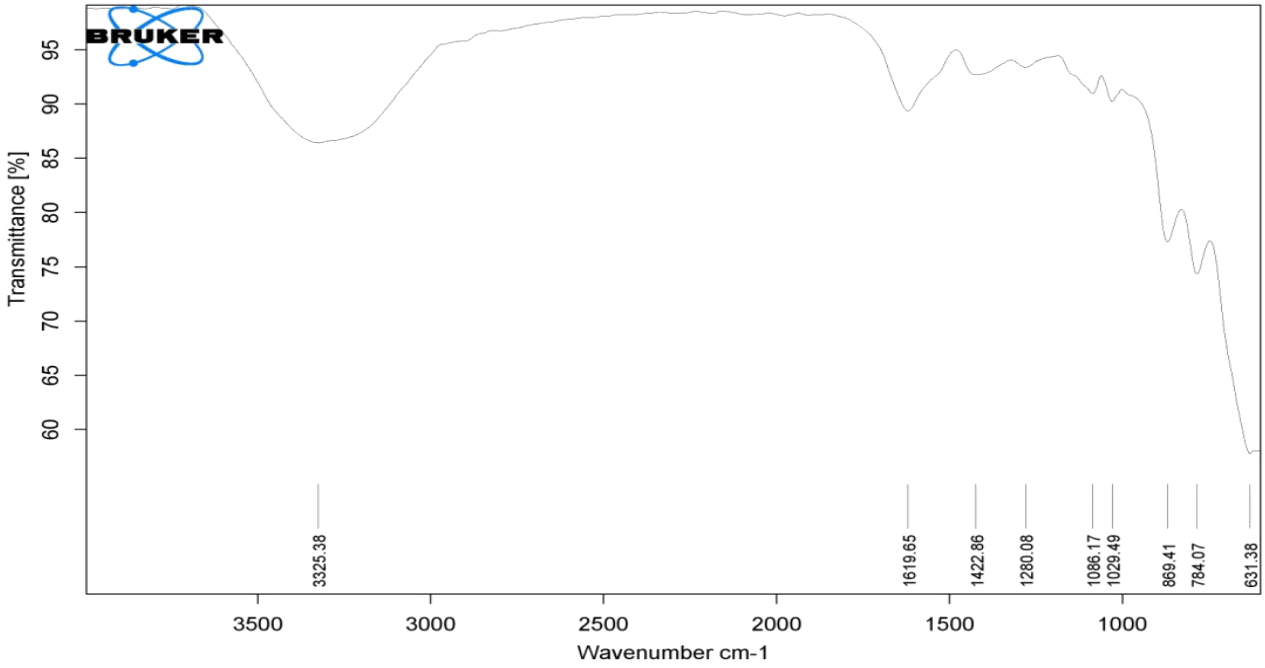

Fig. 2: FTIR spectrum of Fe_3O_4-Ag CSNPs

SEM gave us the clear morphologies of the nanoparticles synthesized. Fe_3O_4-Ag CSNPs when scanned were found to be nearly spherical in shape. The surface area protected by them is also good for adsorption. SEM was recorded in two different stages one before adsorption *i.e.,* after synthesis of the Fe_3O_4-Ag CSNPs and another after adsorption *i.e.,* after the interaction of MO on the surface of Fe_3O_4-Ag CSNPs. From the fig. 3 (a) and (b) we can witness the changes on surface or porosity of the nanoparticles. It is clear from the view that dye molecules get trapped on the surface of nanoparticles and along with the chemical changes, morphological and physical changes also took place.

EDS spectra [fig.4 (a) and (b)] were also recorded for the confirmation of nanoparticles formation, which successfully depicts the elements present. EDS spectra showed the constituents present and the variation of the intensities of the peaks after the MO adsorption also confirms the adsorption process.

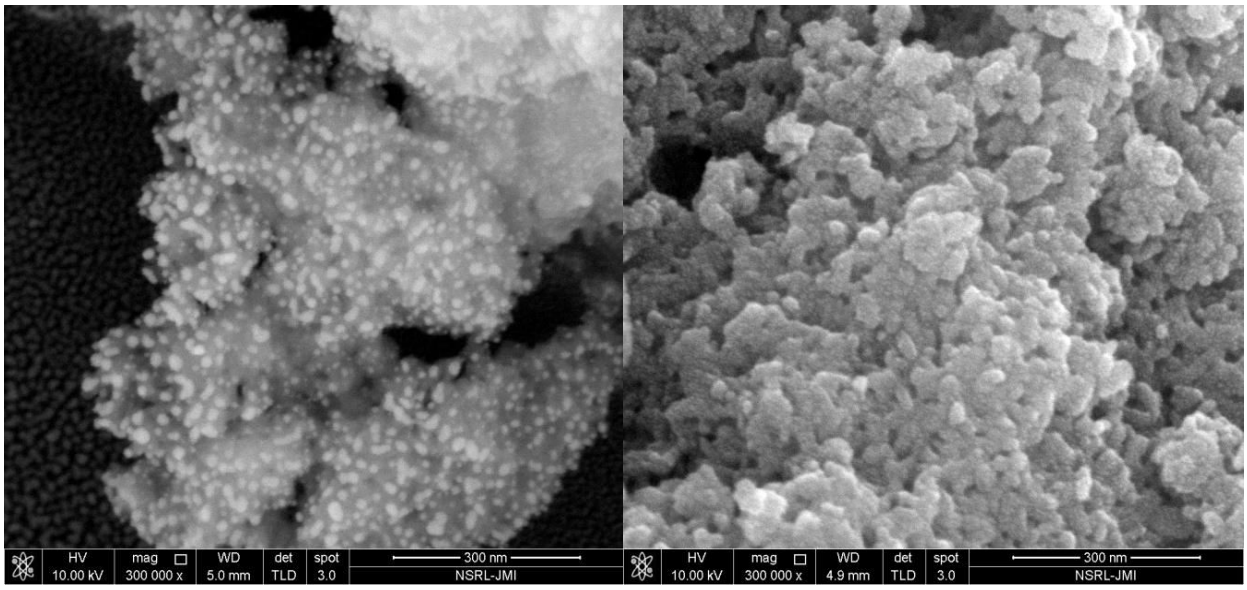

Fig. 3: SEM of Fe_3O_4-Ag CSNPs (a) Before Adsorption, (b) After Adsorption

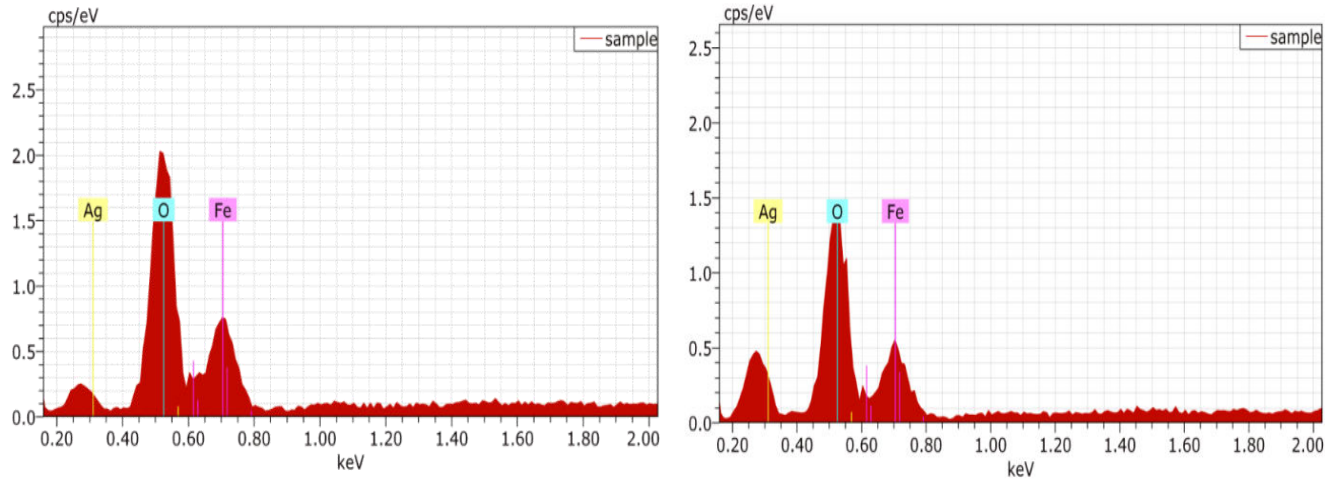

Fig. 4: EDS spectrum of Fe_3O_4-Ag CSNPs (a) Before Adsorption, (b) After Adsorption

To confirm the shape and size of the nanoparticles synthesized TEM was done shown in fig. 5. The shape of the nanoparticles varies from nearly spherical to spherical and the size ranges from 58 nm to 19 nm which is good to provide larger surface area from application point of view.

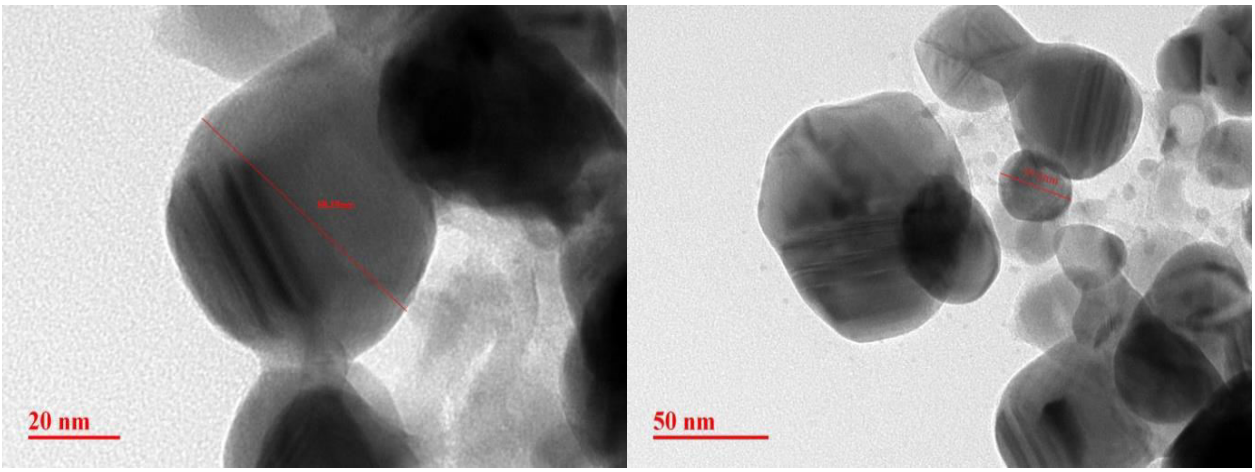

Fig. 5: TEM of Fe_3O_4-Ag CSNPs

3.2. Adsorption Study

3.2.1. Effect of contact time

Graphical presentation of removal efficiency of nanoparticles of MO with variable contact time is shown in fig.6. For maximum uptake of MO by nanoparticles in batch experiment, 1 g of nanoparticles were taken, at pH with 5 ppm MO concentration. Contact time was varied form 30 to 150 min by increasing 30 min at each step, this way 5 readings were taken. This is clear that the percent adsorption increased with increase in contact time and it attains quilibrium at 120 min i.e., no further adsorption taking palce. The percent adsorption increases from 87% to 95%.

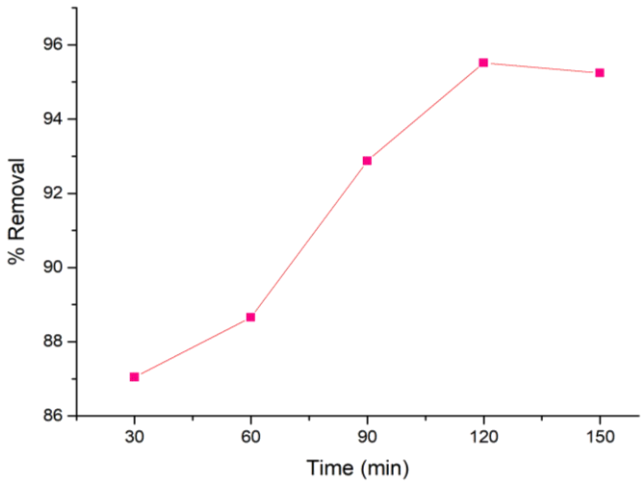

Fig. 6: Variation in adsorption capacity with contact time

3.2.2. Effect of pH

Fig. 7 shows the graphical presentation of removal efficiency of nanoparticles with the increase in pH values. This is clear that maximum adsorption takes place at pH 6. In batch experiment while varying pH, study was performed with constant values of constant time, adsorbate concentration and adsorbent doseas 120 min, 5 ppm and 1 g respectively. Experiment was done by increasing pH from 2 to 10 by increasing the value by the factor of 2 at each step. This is clear that the adsorption increases by increasing pH from 2 to 6 and further adsorption became unfavourable by increasing pH from 6 to 10. Initially percent removal increased from 84% to 92% and then it falls to 77%.

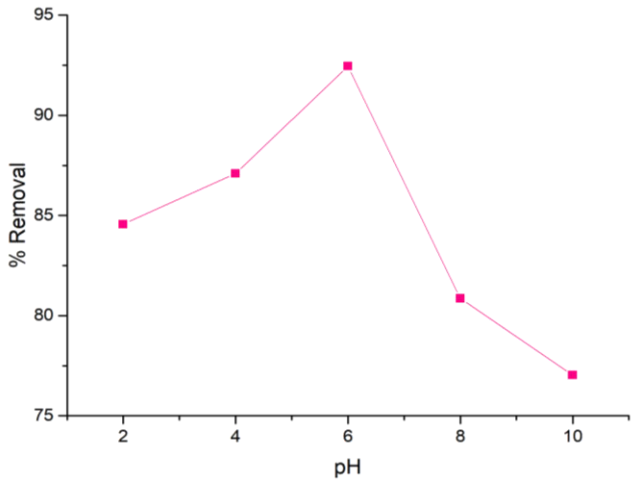

Fig. 7: Variation in adsorption capacity with pH

3.2.3. Adsorbate concentration

Standard solutions of MO were prepared ranging from 1 ppm to 5 ppm, increasing dye concentration by 1 ppm at each step. The experiment was run for 120 min using these 5 dye solutions, pH was set at 6 and 1 g of adsorbent was used. It is clear from the figure 3.8 that

the adsorption capacity decreases with increase in dye concentration from 97%to 78%. This is subjected to the fact that adsorption sites got occupied and none remain left for further adsorption.

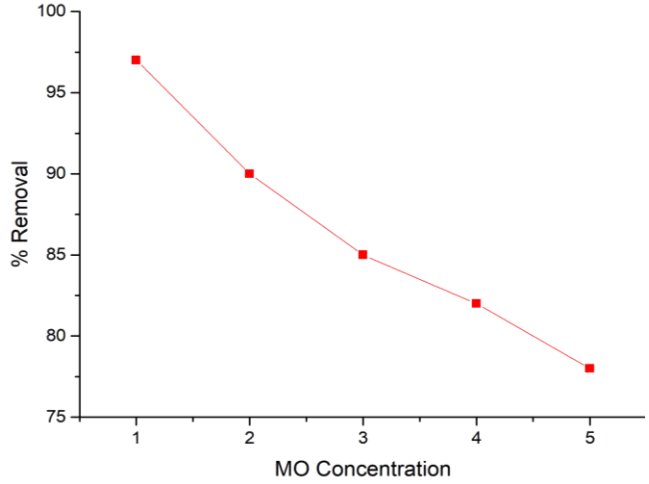

Fig. 8: Variation in adsorption capacity with adsorbate concentration

3.2.4. Effect of adsorbent dose

Adsorbent dose was increased from 1g to 5 g during batch experiment keeping contact time at 120 min, pH at 6 and adsorbate concentration at 5 ppm. It is clear from fig. 9 that adsorption efficiency increases with increase in the adsorbent dose. This is due to the fact that more the adsorbent more is the surface area available for adsorption. The percent removal of dye from aqueous solution increases from 87% to 96% by increasing adsorbent dose.

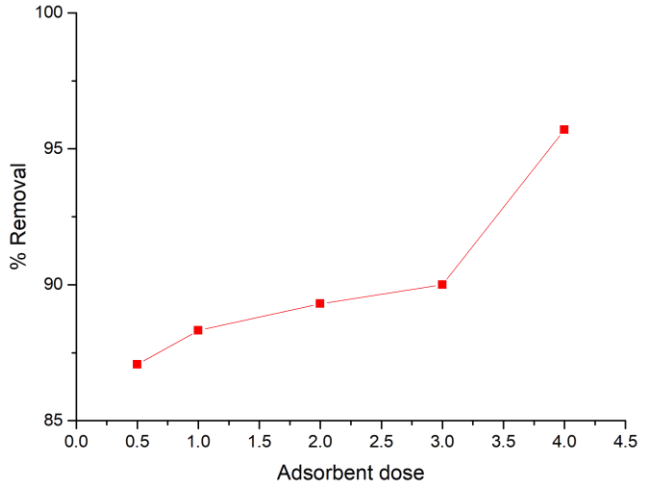

Fig. 9: Variation in adsorption capacity with adsorbent dose

3.2.5. Adsorption isotherm

To propose an efficient dye removal from aqueous solution the data obtained from batch experiment using four variables namely contact time, pH, adsorbate concentration and adsorbent dose was fitted to three different isotherm models. These isotherm models confirm the mechanism that states interaction taking place between adsorbate and adsorbent during adsorption and gives a point where equilibrium is achieved. The mechanistic parameters were evaluated by using Langmuir, Freundlich and Temkin isotherm model. To evaluate the adsorption isotherm to which data is best fitted correlation coefficient (R^2) was calculated.

Langmuir isotherm proposes formation of monolayer of the adsorbate (MO in this case) on the surface of adsorbent (Fe_3O_4-Ag CSNPs) at available sites. Linear form of Langmuir equation can be given as in equation 1.

$$\frac{C_e}{q_e} = \frac{1}{bq_m} + \left(\frac{1}{q_m}\right) C_e \quad \ldots\ldots(1)$$

Whereq_m (mg g^{-1}) represents Langmuir constant (adsorption capacity) and b (L mg^{-1}) is the rate of adsorption, q_e (mg g^{-1}) is the amount of MO adsorbed at the equilibrium and C_e (mg L^{-1}) is the equilibrium concentration.

The linear curve using Langmuir equation is shown in fig. 10. The intercept and slope of the linear curve C_e/q_e versus C_e were calculated which gave the values of Langmuir constants. The values of Langmuir constants q_m, b with $R^2$are given in table 1. The characteristics of Langmuir isotherm can be expressed by separation factor (R_L) which is a dimensionless constant (equation 2). This constant is defined as:

$$R_L = \frac{1}{1+bC_o} \ldots\ldots (2)$$

Where C_o is the initial pesticide concentration (ppm) and b is the Langmuir constant. The value of R_L obtained gives us an idea about the type of Langmuir isotherm: linear ($R_L = 1$), irreversible ($R_L = 0$), favourable ($0 < R_L < 1$) or unfavourable ($R_L > 1$).

In this case the values of R_L were found to be 0.2-0.5 showing the favourable isotherm. It is concluded that Langmuir isotherm is well fitted to the adsorption of MO on Fe_3O_4-Ag CSNPs under the aforesaid maintained conditions.

Equation 3 depicts the linear form of Freundlich isotherm equation as applied to present adsorption system.

$$log\, q_e = log K_f + \frac{1}{n} log C_e \ldots\ldots (3)$$

Where, the Freundlich equilibrium constants, n and K_f, are related to intensity of adsorption and adsorption capacity, respectively. The linear plot of log q_e versus log C_e in fig. 11 gives the values of Freundlich constants by applying simple statistic. The corresponding K_f and n values are reported in table 1 along with R^2 (correlation coefficient) value. The value of n ranging from 1 - 10 represents a favourable adsorption, so in this case Freundlich isotherm is not favourable.

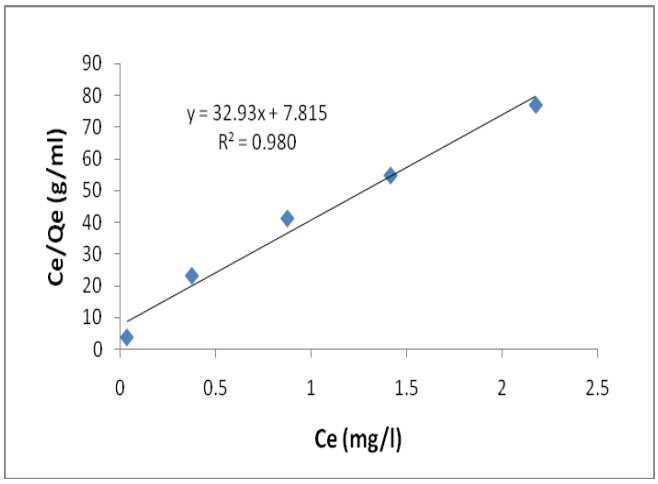

Fig. 10: Langmuir isotherm of MO on Fe_3O_4-Ag CSNPs

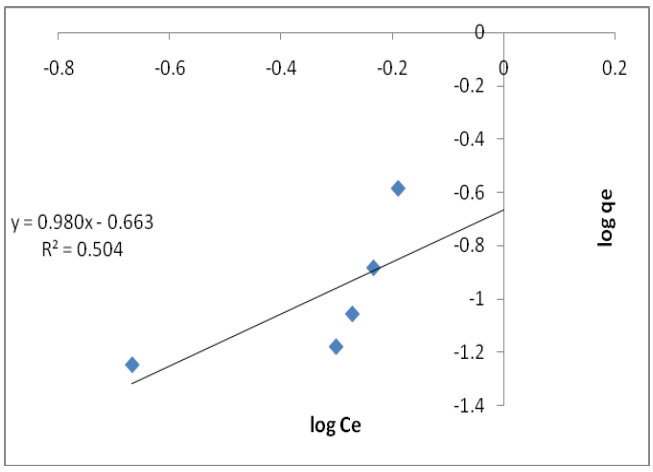

Fig. 11: Freundlich isotherm of MO on Fe_3O_4-Ag CSNPs

To examine the influence of indirect interactions amongst the particles of adsorbate, Temkin adsorption isotherm model (equation 4) was applied. Temkin model suggests that as the surface coverage increases due to the interactions of adsorbate and adsorbent, the heat of adsorption of all the molecules in the layer deceases [47]. The linear form of the Temkin isotherm equation can be given byequation 5.

$$q_e = \left(\frac{RT}{b}\right) LnAC_e \quad \ldots\ldots (4)$$

$$q_e = B \ln A_T + B \ln C_e \ldots\ldots (5)$$

Where A_T (L g^{-1}) is the equilibrium binding constant, b (J/mol) is the heat of adsorption related constant, R is the gas constant (8.314 J/mol/K), and T is absolute temperature (K). The linear plot q_e versus ln C_e in fig.12 gives the values of B and A_T from slopeand intercept, respectively. The values of Temkin constants are given in table 1 along with the correlation coefficient. The plot obtained is not a straight line suggesting non-uniform distribution of binding energy.

Thus, focusing on table 1 it is clear that Langmuir isotherm (R^2 = 0.98) fits well to the adsorption process of MO on Fe_3O_4-Ag CSNPs, whereas the low values for other isotherm model, Freundlich (R^2 = 0.710) and Temkin (R^2 = 0.98) shows poor agreement with the adsorption data.

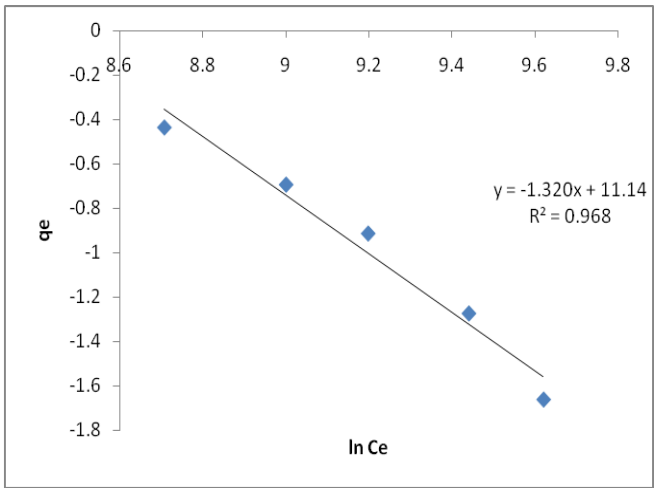

Fig. 12: Temkin isotherm of MO on Fe_3O_4-Ag CSNPs

Table 1: Isotherm model parameters and R^2 value for adsorption of MO onto Fe_3O_4-Ag CSNPs

Dye	Langmuir Model			Freundlich Model			Temkin Model		
	q_m (mg/g)	b (L/mg)	R^2	n	K_f (mg/g)	R^2	A_T (L/g)	B	R^2
Methyl Orange (MO)	0.030	0.237	0.98	0.315	0.500	0.710	.001	-0.451	0.98

3.2.6. Adsorption Kinetics

In order to check out the adsorption process of MO on Fe_3O_4-Ag CSNPs, three kinetic models namely, including pseudo-first-order, pseudo-second-order and intra-particle diffusion model were used. The procedure used for equilibrium tests to fit in isotherm models was used for kinetic tests as well. The aqueous solution of dye with fixed concentration, dose and pH was taken and the concentration was measured at the time interval of 30 min. The amount of dye adsorbed; q_t (mg g^{-1}), at the surface of Fe_3O_4-Ag CSNPs at time; t, was calculated usingequation 6.

$$q_t = \frac{C_o - C_t \times V}{C_o \times W} \ldots\ldots (6)$$

The pseudo-first-order equation proposed by Lagergren and Svenska as given byequation 7 was used to determine the rate constant of adsorption.

$$\ln(q_e - q_t) = \ln q_e - k_1 t \ldots\ldots (7)$$

where q_e and q_t (mg g^{-1}) are the amounts of pesticide adsorbed at equilibrium and time, t (h) and k_1 (h^{-1}) is the adsorption rate constant. To calculate the values of k_1 and q_e by using pseudo-first-order kinetics plot of ln (q_e - q_t) versus t for the initial 5ppm concentration of the pesticide was drawn, which has been presented in fig. 13. The values of kinetic parameters from equation 7 along with correlation coefficient are given in table 2.

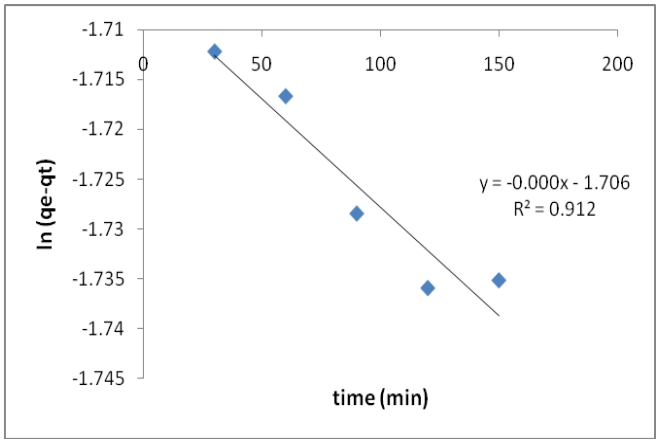

Fig. 13: Pseudo-first-order kinetics of MO on Fe_3O_4-Ag CSNPs

Table 2: Rate constants of Pseudo-first-order and pseudo-second-order for adsorption of MO onto Fe_3O_4-Ag CSNPs

Dye	q_e expt (mg/g)	Pseudo-first-order			Pseudo-second-order		
		q_e (mg/g)	k_1	R^2	q_e (mg/g)	k_2	R^2
Methyl Orange (MO)	0.049	0.182	0.0002	0.955	0.049	3.925	1

The pseudo-second-order kinetics for equilibrium adsorption can be given by equation 8.

$$\frac{t}{q_t} = \frac{1}{k_2 . q_e^2} + \frac{1}{q_e} t \ldots. (8)$$

Where k_2 (g mg^{-1} h^{-1}), is the rate constant of second-order adsorption. To calculate the values of q_e and k_2 by using pseudo-second-order kinetics, plot of t versus t/q_t are presented in fig. 14. The values of kinetic parameters from equation 8 are given in table 2. It is clear that the correlation coefficient for pseudo-second-order is greater than that of pseudo-first-order and the experimental q_e value agrees with the observed q_e value of pseudo-second-order equation. This adsorption process therefore, follows pseudo-second-order kinetics.

Weber and Morris proposed an intraparticle diffusion model to identify the diffusion mechanism of adsorption. According to this model adsorbate uptake varies proportional to $t^{1/2}$and not to the contact time t [48]. Equation 9 which is given below represents the linear form of the intraparticle diffusion model.

$$q_t = K_{id} t^{1/2} + I \ldots\ldots (9)$$

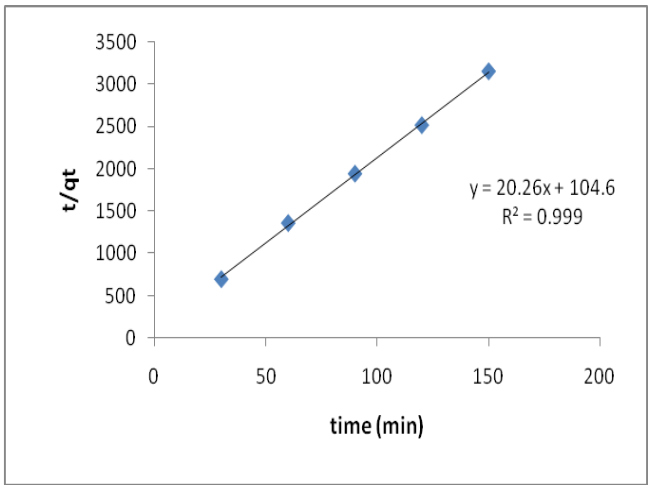

Fig. 14: Pseudo-second-order kinetics of MO on Fe_3O_4-Ag CSNPs

Where K_{id} is the intraparticle diffusion rate constant and I is the thickness of the boundary layer. The plot of q_t versus $t^{1/2}$shown in figure 3.15, gives the value of K_{id} and I from, slope and intercept, respectively. Figure 3.15, shows multistage linearity involving moderate

diffusion rate at the initial stage, followed by rapid diffusion, indicating that the intra-particle diffusion is the rate controlling adsorption process [49-50].

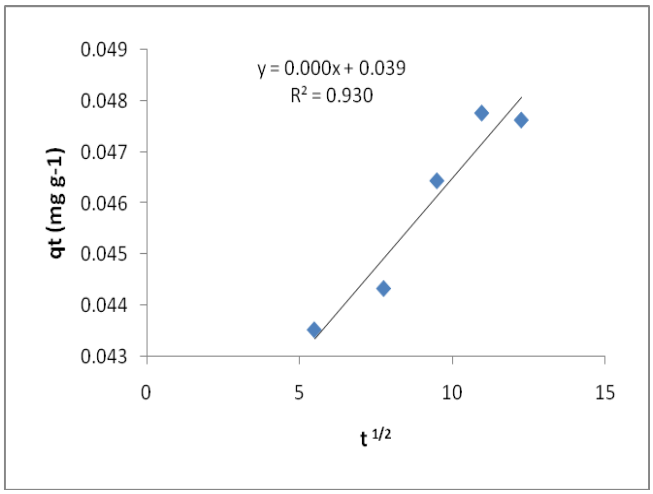

Fig. 15: Weber and Morris diffusion model of MO on Fe_3O_4-Ag CSNPs

4. CONCLUSION

In this study, aqueous extract of *Cinnamomum verum* bark was used for the green synthesis of Fe_3O_4-Ag CSNPs. The synthesized nanoparticles were characterized by using various advance techniques like UV-Vis spectroscopy, FTIR spectroscopy, SEM, EDS and TEM. SEM revealed that particles are nearly spherical in size which was further confirmed by TEM indicating that the nanoparticles are spherical in shape and the size ranges from 19nm to 58 nm.

The Fe_3O_4-Ag CSNPs showed good adsorption quality. Batch experiments were conducted to find out the capability and mechanism of adsorption with these nanoparticles. MO was taken as an adsorbate which is a well known pollutant in today's scenario. In the batch experiments, equilibrium was achieved within 120 min of reaction time. The percent removal of pesticide in 120 min with variable dose increased from 87% to 92%. The maximum removal of pesticide occured at pH 6. On varying the initial concentration from 1-5 mg L^{-1} the percent removal deceases from 97% to 78% as the number of vacant sites for adsorption become less. Out of three isotherm models, Langmuir isotherm model (R^2 = 0.98) fitted best to the adsorption process, as compared to Freundlich isotherm (R^2 = 0.71) and Temkin isotherm (R^2 = 0.98) model. Langmuir model suggests that the formation of a monolayer of MO takes place at the surface of Fe_3O_4-Ag CSNPs. Pseudo-second-order kinetics explained the adsorption process better than pseudo-first-order. It can, therefore, be concluded that, the Fe_3O_4-Ag CSNPs which are easily synthesized can be used as an efficient and eco-friendly adsorbent for the removal of dye from aqueous solution.

5. ACKNOWLEDGEMENT

One of the authors Priya Kumari is thankful to UGC (University Grant Commission), New Delhi, India for financial assistance by providing Non-NET fellowship.

Conflict of interest

None declared

Source of funding

None declared

6. REFERENCES

1. Crini G. *Bioresource Technology*, 2006; **97**:1061-1085.
2. Gregory AR, Elliott J, Kluge P. *Journal of Applied Psychology*, 1981; **1**:308-313.
3. Sivaraj R, Namasivayam C, Kadirvelu K. *Waste Management Volume*, 2001; **21**:105-110.
4. Chen KC, Wu J, Huang C, Liang Y, Hwang SJ. *Journal of Biotechnology*, 2003; **101**:241-252.
5. Gupta VK, Mittal A, Jain R, Mathur M, Sikarwar S. *Journal of Colloid and Interface Science*, 2006; **303**:80-86.
6. Gupta VK, Jain R, Varshney S. *Journal of Hazardous Materials*, 2007; **142**:443-448.
7. Gupta VK, Ali I, Saini VK. *Journal of Colloid and Interface Science*, 2007; **315**:87-93.
8. Gupta VK, Mittal A, Gajbe V, Mittal J. *Journal of Colloid and Interface Science*, 2008; **319**:30-39.
9. Cheremisinoff NP. Handbook of Water and Wastewater Treatment Technologies. 1st ed. Boston: Butterworth-Heinemann; 2002.
10. Marmagne O, Coste C. *American Dyestuff Reporter*, 1996; **85**:15-20.
11. Shi BY, Li GH, Wang DS, Feng CH, Tang HX. *Journal of Hazardous Materials*, 2007; **143**:567-574.
12. Wang M, Li H, Wu J,Huo Y,Guo G, Cao F. Flocculant for purification of printing and dyeing wastewater. UnivShanghai Normal, 2006.
13. Zhou Y, Liang Z, Wang Y. *Desalination*, 2008; **225**:301-311.

14. Gupta VK, Jain R, Varshney S. *Journal of Colloid and Interface Science*, 2007; **312**:292-296.
15. Lin SH, Peng CF. Water Research, 1994; **28**:277-282.
16. Gupta VK, Mittal A, Gajbe V. *Journal of Colloid and Interface Science*, 2005; **284**:89-98.
17. Bansal RC, Goyal M. Activated Carbon Adsorption. Boca Raton: Taylor & Francis Group 2005.
18. Danis TG, Albanis TA, Petrakis DE, Pomonis PJ. *Water Research*, 1998; **32**:295-302.
19. Freeman HM. Standard Handbook of Hazardous Waste Treatment and Disposal, 2nded. New York: McGraw-Hill Education; 1989.
20. Imamura K, Ikeda E, Nagayasu T, Sakiyama T, Nakanishi K. *Journal of Colloid and Interface Science*, 2002; **245**:50-57.
21. Liapis AI. Fundamentals of Adsorption. New York: Engineering Foundation;1987.
22. Mantell CL. In: Adsorption. 2nd ed. New York: McGraw-Hill Book Company, Inc; 1951.
23. Mattson JS, Mark HBJ. Activated Carbon Surface Chemistry and Adsorption from Solution. New York: Marcel Dekker, Inc; 1971.
24. Pirbazari M, Badriyha BN, Miltner RJ. *Journal of Environmental Engineering*, 1991; **117**:80-100.
25. QuignonF, Thomas F, Gantzer C, Huyard A, Schwartzbrod L. *Water Research*, 1998; **32**:1222-1230.
26. Weber JrWJ, Hopkins CB, Bloom JrR. Journal*(Water Pollution Control Federation)*, 1970; **42**:83-89.
27. Kuppusamy P, Yusoff MM, Maniam GP, Govindan N. *Saudi Pharmaceutical Journal*, 2016; **24**:473-484.
28. Chen D, Qiao X, Qiu X, Chen J. *Journal of Materials Science*, 2009; **44**:1076-1081.
29. Wang H, Wei Q, Wang X, Gao X, Zhao X. *Fibers and Polymers*, 2008; **9**:556-560.
30. Kim L, Jun K, Sung WS, Moon SK, Choi JS, Kim JG. *Journal of Microbiology and Biotechnology*, 2008; **18**:1482-1484.
31. Lee HJ, Yeo SY, Jeong SH. *Journal of Material Science*, 2003; **38**:2199-2204.
32. Lakshmanan G, Sathiyaseelan A, Kalaichelvan PT, Murugesan K. *International Journal of Modern Science*, 2018; **4**:61-68.
33. Makarov VV, Love AJ, Sinitsyna OV, Makarova SS, Yaminsky IV, Taliansky ME, Kalinina NO. *ActaNaturae*, 2014; **6**:35-44.
34. Iravani S. *Green Chemistry*, 2011; **13**:2638-2650.
35. Cotolan N,Rak M, Bele M, Cör A, Muresan LM, Milošev I. *Surfaceand Coatings Technology*, 2016; **307**:790-799.
36. Wing CG, Esparza R, Hernandez CV, Garciaand MEF, Yacaman MJ. *Nanoscale*, 2012; **4:**2281-2287.
37. Magnusson MH, Deppert K, Malm JO, Bovin JO,Samuelson L.*Nanostructure Material*, 1999; **12**:45-48.
38. Zhu J, Shi J, Pan Y, Liu X, Zhou L. *Journal of Natural Science*, 2013; **18**:530-534.
39. Thomas R, Nair AP, Kr S, Mathew J, Ek R. *Applied Biochemistry and Biotechnology*, 2014; **173**:449-460.
40. Kumar PPNV, Pammi SVN, Kollu P, Satyanarayana KVV, Shameem U. *Industrial Crops and Products*, 2014; **52**:562-566.
41. Zuckerman MM, Molof AH, Weber WJ. *Journal (Water Pollution Control Federation)*, 1970; **42**: 437-463.
42. Guzm´an MG, Dille J, Godet S. *International Journal Chemical and Biomolecular Engineering*, 2009; **2**:104-11.
43. Fei X, Jia M, Du X, Yang Y, Zhang R, Shao Z, Zhao X, Chen X. *Biomacromolecules*, 2013; **14**:4483-4488.
44. Panacek A, Kolar M, Vecerova R, Prucek R, Soukupova J, Krystof V, *et al*. *Biomaterials*, 2009; **30**:6333-6340.
45. Seger C, Godejohann M, Tseng LH, Spraul M, Girtler A, Sturm S, Stuppner H. *Analytical Chemistry*, 2005;**77**:878-885.
46. Fayaz AM, Balaji K, Girilal M, Yadav R, Kalaichelvan PT, Venketesan R. *Nanomedicine: Nanotechnology, Biology and Medicine*, 2010; **6**:103-109.
47. Gupta VK, Mittal A, Jhare D, Mittal J. *Royal Society of Chemistry Advanced*, 2012; **2**:8381-8389.
48. Ansari FA, Alam M. *International Journal of Applied Research*, 2014; **4:**439-442.
49. Bakouri HE, Usero J, Morillo J, Rojas R, Ouassini A. *Bioresource Technology*, 2009; **100:**2676-2684.
50. Bakouri HE, Usero J, Morillo J, Ouassini A. *Bioresource Technology*, 2009; **100**:4147-4155.